JOURNAL OF PROPULSION AND POWER
Vol. 21, No. 5, September–October 2005

Design and Implementation of Feedback Control for Counterflow Thrust Vectoring

Yanan Zhao,* Emmanuel G. Collins Jr.,† Farrukh Alvi,‡ and Delfim Dores§
Florida A&M University and Florida State University, Tallahassee, Florida 32310

Aircraft thrust vector control is currently implemented using movable control surfaces such as vanes and flaps. Counterflow thrust vectoring (CFTV) is a fluidic approach to thrust vectoring that has the potential to improve on the conventional approaches by reducing weight and increasing the reaction speed. Open-loop implementation of CFTV has been demonstrated in laboratory settings. However, ultimately this technology must be implemented using feedback control. The primary control objective is to achieve fast slew rates by compensating for the transportation delay and parameter uncertainties. The paper describes an experimental test bed for investigating feedback control of CFTV. System estimation results based on open-loop test data are presented. This paper then develops a PID control law, which is sometimes implemented with a Smith predictor to compensate for the transportation delay and/or an antiwindup scheme to compensate for actuator saturation. The control laws are experimentally demonstrated, and their performance is compared using different types of reference signals.

Introduction

THE maneuverability of aircraft is traditionally achieved by the use of aerodynamic control surfaces such as ailerons, rudders, elevators, and canards. The deflection of these surfaces modifies the exterior shape of the vehicle at critical points of its structure, thus creating a change in the aerodynamic forces acting on the vehicle and causing it to maneuver.[1,2]

Thrust vector control (TVC) is a more recent technology that increases vehicle maneuverability by directly changing the direction of the thrust force vector. This approach has been successfully implemented on several military aircraft and has resulted in increased roll rates and enhanced maneuverability at low-speed, high-angle-of-attack flight conditions, in which aerodynamic surfaces are very ineffective. TVC can also reduce the distance necessary for take-off and landing or even make vertical take off and landing possible.

Current implementation of TVC employs movable control surfaces such as vanes and/or flaps arrayed around the nozzle exit to redirect the jet exhaust. The mechanical actuators and linkages used to change the thrust vector angle add weight and complexity to the aircraft, which lead to increased cost and maintenance requirements. In addition, the dynamic response of the jet is limited by the response of the mechanical actuators used, and the thrust losses are not small.[1–3] A promising alternative approach is fluidic thrust vectoring, where secondary airflows are employed to redirect the primary jet. Fluidic thrust vectoring requires few or no moving parts in the primary nozzle; therefore, it simplifies the hardware and reduces weight and maintenance needs. In addition, it has the fast dynamic response inherent to fluidic devices.[2–4]

Counterflow thrust vectoring (CFTV) was first proposed by Strykowski and Krothapalli.[5] This technique is different than previously proposed fluidic techniques. Instead of having a secondary airstream inside the nozzle, CFTV uses a secondary flow traveling in the opposite direction to that of the primary jet outside the primary nozzle. Recent engineering research has successfully demonstrated the potential of thrust vector control using counterflow at conditions up to Mach 2 (Refs. 1, 4, and 6). However, because fluidic concepts in general are bistable and hysteretic in nature, CFTV has some limitations. In particular, for certain CFTV geometries the primary jet tends to attach itself hysteretically to the suction collar at certain conditions. When this occurs, control of the thrust vectoring angle is lost. This attachment is difficult to overcome without large changes in flow conditions.[3] A jet with a design Mach number 2 was used in this research because considerable experimental results are available to the authors at this Mach number. However, counterflow thrust vectoring has also been demonstrated at other Mach numbers, for example, Mach number 1.4 as well as for subsonic flow.[2,6]

Past studies of CFTV have focused exclusively on the open-loop behavior. However, for practical implementation it is vital that the counterflow scheme be used in conjunction with feedback. Hence, the primary objective of the research reported here is to design and implement effective feedback control laws for CFTV. Figure 1 illustrates that the CFTV feedback control loop constitutes an important minor loop of the overall aircraft attitude control. The control system must achieve fast slew rates by compensating for the transportation delay in the presence of significant parametric uncertainty. In addition, for certain CFTV geometries it must be able to compensate for the hysteresis that occurs when the counterflow is effectively stopped at attachment. Hysteresis is a nonlinearity for which traditional control methods are insufficient.[7] However, CFTV can be continuously controlled over a wide range of operating conditions. Hence, in this paper control law design is developed assuming hysteresis does not occur. The design objective here is then to obtain fast slew rates in the presence of time delay and parametric uncertainty.

PID control and its variations (P, PI, or PD) is the most commonly used control law in process control applications for the compensation of both delayed and nondelayed processes.[8] PID controllers often display robustness to incorrect process model order assumptions and limited process parameter changes. As the detailed physics of CFTV system are not entirely understood, a PID controller was developed based on a model estimated using experimental open-loop data. A Smith predictor was used in conjunction with PID control to compensate for the effects of time delay while an antiwindup scheme was used to compensate for actuator saturation.

The paper is organized as follows. The second section describes some of the details of the CFTV concept along with the experimental test bed developed for feedback control development. The third section presents system modeling and analysis results. The fourth section develops a PID control law and shows how it can be used in conjunction with a Smith predictor and/or an antiwindup scheme and gives some closed-loop simulation results. The fifth section

Received 17 August 2004; revision received 16 March 2005; accepted for publication 31 March 2005.

*Research Associate, Department of Mechanical Engineering.
†John H. Seely Professor, Department of Mechanical Engineering.
‡Associate Professor, Department of Mechanical Engineering. Member AIAA.
§Ph.D. Student, Department of Mechanical Engineering.

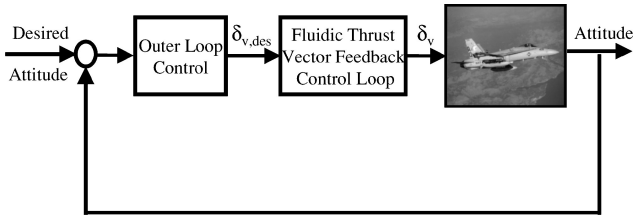

Fig. 1 Aircraft attitude control using fluidic thrust vector control.

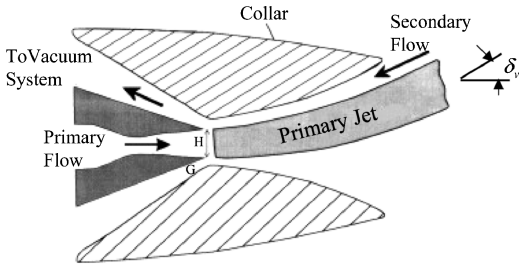

Fig. 2 Schematic of counterflow thrust vector control.

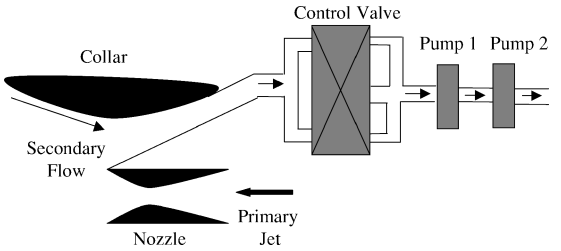

Fig. 3 Schematic functional diagram of the test bed.

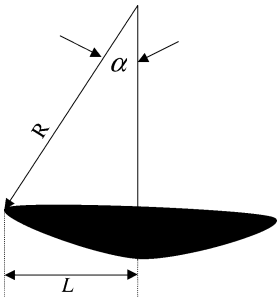

Fig. 4 Collar.

presents experimental results. Finally, the sixth section presents conclusions.

Description of CFTV and the Experimental Test Bed

In this section, the concept of CFTV is described, and an experimental test bed for investigating feedback control of CFTV is presented.

Counterflow Thrust Vectoring

The basic geometry of a CFTV device used for pitch vectoring is illustrated in Fig. 2. The collars are placed on either side of the primary flow nozzle (top and bottom in the figure) creating gaps between the exhaust jet and the collar surfaces, which are curved away from the jet axis in the streamwise direction. To achieve upward thrust vectoring at an angle δ_v, for example, a secondary counterflow must be established between the primary jet and the upper collar surface, creating a continuous flow path between the surrounding ambient fluid and the vacuum system. The action of counterflow in the upper shear layer gives rise to asymmetric entrainment and a cross-stream pressure gradient sufficient to vector the jet.[4] When the vacuum system is activated, creating counterflow in the gap between the jet and the collar, continuous thrust vectoring can be achieved.[4] Previous experimental studies have demonstrated continuous control for values of δ_v up to 20 deg (Ref. 2). In this figure, G represents the gap height, and H is the nozzle height.

It is important to recognize that the thrust vectoring angle cannot be directly measured in practical implementation of CFTV, although experimental techniques do allow its measurement in laboratory settings. However, it has been shown that the pressure parameter $\Delta P_G A_{\text{side}}/\rho U^2 A_{\text{jet}}$, which is essentially a nondimensional ratio of the side force acting on the collar and the axial force imposed by the jet, has a nearly linear relationship to the thrust vector angle over a wide range of conditions (see Fig. 9 of Ref. 4). Here, P_G is the pressure established in the secondary stream as measured in the jet exit plane on the collar surface, ΔP_G is the static negative gauge pressure in the jet exit plane on the collar surface (i.e., $\Delta P_G = P_{\text{atm}} - P_G$, where P_{atm} represents the absolute atmospheric pressure), A_{side} is the collar side area, ρ is the primary jet density, U is the primary jet velocity, and A_{jet} is the jet area at the nozzle exit. Thus, in practice ΔP_G will be selected as the command variable.

For certain CFTV geometries, if the pressure on the collar wall drops too much (i.e., ΔP_G becomes very large), the deflection of the jet will be too severe, and it will attach to the wall. If this happens, continuous control of the jet is compromised because at this time thrust vectoring angle would generally jump to a value near the collar terminal angle. Jet attachment is a hysteretic phenomenon because once the jet is attached to the collar, changes in the secondary flow have little effect on the thrust vectoring angle, and simply reducing the counterflow rate to reduce ΔP_G back to the value at which jet attachment occurred is not sufficient to release the jet from the collar.[3] Feedback control of CFTV in the presence of hysteresis in beyond the scope of this paper.

Experimental Test Bed

To investigate feedback control of CFTV, a test bed has been successfully set up in the Fluid Mechanics Research Laboratory at the Florida A&M University and Florida State University College of Engineering. The characteristics of the current experiment have been shown to match those in the literature.[2,4]

The experimental test bed consisted of five major parts: a jet, a collar, a control valve, two pumps, and the pipe connections. A schematic functional diagram of the test bed is shown in Fig. 3. Notice that for simplicity only one collar was used. Hence, the experiment allows only positive pitch angles δ_v.

The rectangular Mach 2 jet in the exit plane has a width of 32.5 mm and a height of 5 mm. The inner contour of the collar is an arc of constant radius of curvature swept through an angle α and extending downstream of the nozzle exit for a distance given by $L = R \sin\alpha$, where $L = 34$ mm, $R = 78.5$ mm, and $\alpha = 25.6$ deg (see Fig. 4).

The forward stream to the jet is supplied by a high-displacement reciprocating compressor, which is capable of supplying air at a maximum storage pressure of 160 bars. The vacuum source for the counterflow is provided by two Fuji VFC804A-7W pumps mounted downstream of the test rig. The two pumps can be connected in series as shown in Fig. 3, or they can be used separately, that is, either of the pumps can be disconnected from the test bed.

To implement feedback control, a control valve is installed between the collar and pumps to control the counterflow, which determines the thrust vector angle. A model 27N pneumatic R-DDV servovalve from HR Textron is used in the test rig for this purpose.

Data acquisition and control are implemented using dSPACE, which consists of a DS2002 A/D board, a DS2102 D/A board, a DS1005 PPC board, and a PX10 expansion box. To monitor the jet pressure (which should be 115 psi for a Mach 2 jet), a Validyne multiple range pressure transducer (model DP15TL) is used. There are 11 static-pressure taps along the collar wall, and the multiple pressure measurements required to determine the collar static-pressure distribution are facilitated by a Scanivalve model OED2 pressure sampling scanner.

System Modeling and Analysis

Although the general principles responsible for CTFV, that is, increased entrainment as a result of counterflow are known (see

Refs. 1 and 4 and for details), the detailed physics of CFTV are not entirely understood; thus, it is difficult to build a CFTV model using first principles. In this section, system modeling and parameter estimation were performed based on open-loop tests.

Open-Loop Tests and System Modeling

The model required for feedback control design has the voltage to the control valve as the input and the command variable ΔP_G as the output. To study the system characteristics under different operating regions, the CFTV test bed has been extensively tested for step inputs with amplitude $1, 2, \ldots, 5$ V. (The range of the control valve voltage is [0, 5] V.) To capture the transient performance of the system clearly, the step signals were applied at $t = 10$ s. One set of resulting step responses is shown in Fig. 5.

The tests were performed with both the first and second vacuum pumps on and a geometry ratio of $G/H = 0.38$. The sampling rate was chosen as $T_s = 0.01$ s. Because of the installation of collar at the exit of jet engine, thrust vectoring exists with even a fully closed control valve. To consider only the effect of the control valve, open-loop response curves representing $-[P_G(t > 10\text{ s}) - P_G(t = 10\text{ s})]$ were plotted as shown in Fig. 6. A negative sign is used because a higher control valve signal always results in lower gap pressure along the collar.

By observing the open-loop step responses of the system, second-order models were constructed to represent the system dynamics. The second-order models with time delay are of the form, $(K/T^2s^2 + 2T\xi s + 1)e^{-Ls}$, where K is the gain, T is the time constant, ξ is the damping ratio, and L is the time delay of the system. Experimental open-loop methods for parameter estimation have been widely studied.[9] A method proposed by Huang and Chou,[10] a five-point method, was used to estimate the process parameters. The estimated parameters under five different control valve voltage inputs are listed in Table 1.

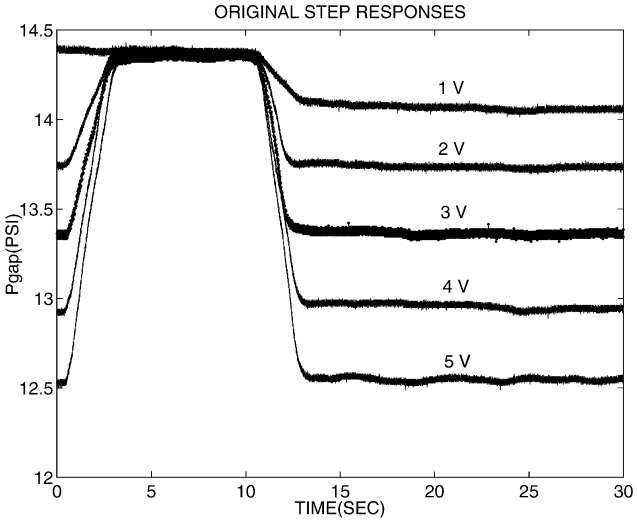

Fig. 5 Open-loop step responses under different control valve voltage.

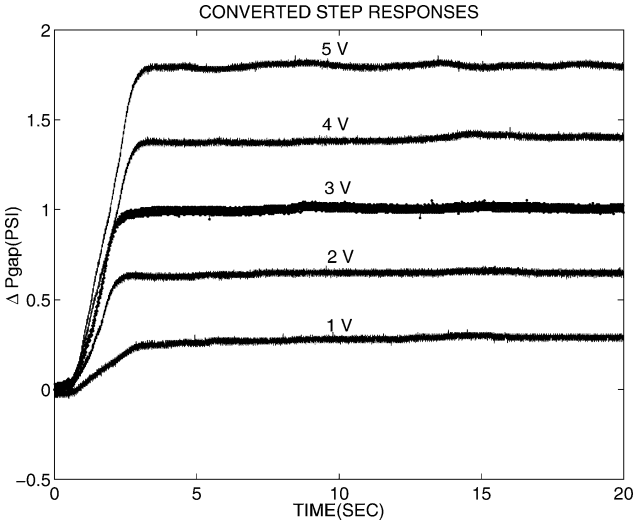

Fig. 6 Converted open-loop step responses under different control valve voltage.

Table 1 Model estimation at different input values

Input amplitude, V	K	T, s	ξ	L, s
1	0.2889	0.6681	0.9181	0.5440
2	0.3258	0.5089	0.8650	0.5543
3	0.3365	0.5033	0.8504	0.5730
4	0.3501	0.6420	0.8626	0.5458
5	0.3602	0.6675	0.8372	0.5694
Average value	0.3323	0.5980	0.8667	0.5573

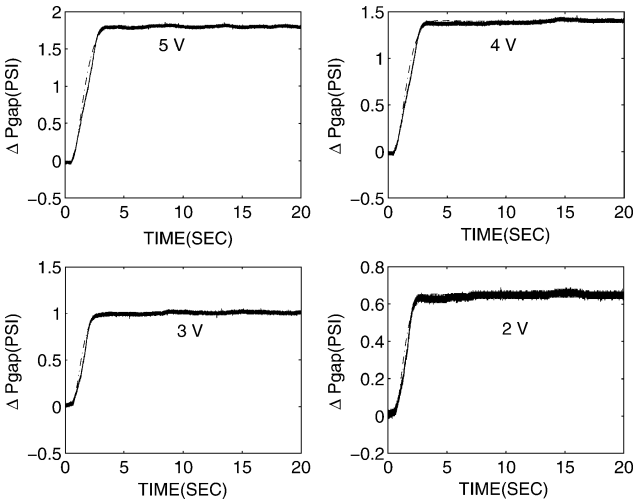

Fig. 7 Comparison of test response (——) and system estimated response (– – –).

Figure 7 compares the simulated step responses based on the estimated models and the test data under different control valve voltages. It is seen that a second-order plus time-delay model closely matches the time delay and the steady state. However, the estimated model has a slightly faster rise time than the test data because the dashed lines in Fig. 7 arrive at their steady-state values slightly faster than the solid lines.

As shown in Table 1, under different control valve inputs the parameters of the second-order models had different values. The gain K varied within 13.06% of its average value, the time constant T varied within 15.84% of its average value, the damping ratio ξ varied within 5.93% of its average value, and the time delay L varied within 2.82% of its average value. The parametric variations at different operating points are assumed to be caused by nonlinearities in the control valve and fluid dynamics.

Additional Sources of Uncertainty in the CFTV System

The CFTV system suffers from additional sources of uncertainty. Two of the major sources are described next.

The dynamics of CFTV changes along with the power level of the pumps. For example, the running temperature of the pumps affects their efficiency and thereafter the CFTV dynamics. A colder pump is more efficient and hence produces higher counterflow. Usually, the gap pressure obtained with a colder pump is lower than that of a warmer pump. An intercooling system is desired to keep the pump running at peak efficiency; however, it is not used in the current experiment.

The dynamics of CFTV also changes along with ambient conditions. For example, the temperature of the air supplied to the jet affects the performance of CFTV system. The air source of the

Table 2 Gains obtained with another set of open-loop test data

Input amplitude, V	K
1	0.3500
2	0.3352
3	0.3171
4	0.3232
5	0.3401
Average	0.3331

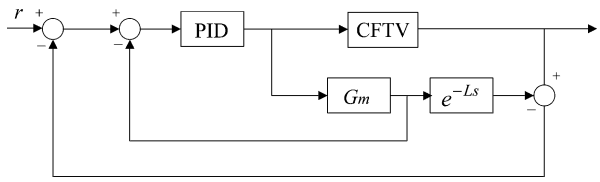

Fig. 8 Block diagram of a Smith predictor.

compressor is the atmosphere air. Because of the variation of atmospheric temperature, the temperature of the air supplied to the jet engine is not guaranteed. The temperature change causes the performance variation of the primary flow and thereafter the collar pressure.

Another set of open-loop tests was performed to illustrate the preceding uncertainty. It was also conducted with both the first and second vacuum pumps on and a geometry ratio of $G/H = 0.38$ as was the case corresponding to the tests of Table 1. However, though not explicitly recorded, the ambient temperature for this set was different. (This test set was conducted on the afternoon of 14, April 2004, whereas the test set corresponding to Table 1 was conducted on the morning of 3 March 2004.) In addition, the power level of the pumps varied for the two experiments. The gains obtained with the second experiment are shown in Table 2. It is seen that these values are significantly different from those shown in Table 1.

PID Controller Design

After the CFTV system model was obtained, feedback control laws were designed to control ΔP_G and thus the counterflow thrust vector angle δ_v. To increase the ability to maneuver the vehicle quickly, one control objective is to have a fast slew rate. In addition, to ensure smooth motion, it is desired to avoid system overshoot. These objectives must be accomplished in the presence of substantial parametric variation and system delay. Control valve saturation is also a significant obstacle. PID controllers are the most commonly used controllers in industrial practice.[8] PID control was used here because of its simple structure, ease of design and robustness under certain model and parameter uncertainties. A Smith predictor was used along with PID control to compensate for the system delay. An antiwindup strategy was used to compensate for actuator saturation.

PID Control Using Tuning Rules

Many PID tuning rules are available for a second-order system with time delay.[11] A direct synthesis method proposed by Miluse etc.[11] was used to obtain the PID gains. For 0% overshoot, the proportional gain, the integral time constant, and derivative time constant of the PID controller can be computed as $K_p = 0.736(\xi T/KL)$, $T_i = 2\xi T$, and $T_d = 0.5T/\xi$.

In the first design attempt, the variation of the system dynamics was neglected, and only one PID controller was designed for the entire operating region of the system. Thus, the model parameters were taken as the average of the corresponding parameters as given in Table 1. The gains of the obtained PID controller are $K_p = 2.0615$, $K_i = 1.9872$, and $K_d = 0.7106$. The controller demonstrated its robustness during experimental implementation.

Smith Predictor

As just described, open-loop system tests revealed the existence of transportation delay in the CFTV system. A Smith predictor is an effective tool for compensating for system time delay. As shown in Fig. 8, the basic idea of the Smith predictor is to use a delay-free model of the process dynamics G_m to predict the effect of current control actions on the actual delayed process output. Additional feedback from the actual process output is then used to compensate for modelling error and process disturbances.[12–14] Here, the primary controller used in the Smith predictor is the PID controller just designed.

Note that the Smith predictor is very dependent on the system model. To cope with the process parameter variation, an adaptive Smith predictor using online parameter estimation or robust tuning is preferred.[12,14] In the current implementation, G_m is taken as the average dynamics model.

Antiwindup

The working range of the control valve is within [0 5] V. It was observed that for the PID controller control valve saturation occurred at higher setpoints at which the generated control signal was higher than 5 V. Saturation also occurred at the instant of dramatic setpoints change, where a big change of control signal was produced to track the change of setpoint. In addition, saturation occurred in the case of abnormal sensor noise.

The performance of PID control can be severely deteriorated in practical cases by the presence of saturation of the actuators, which causes the well-known phenomenon of integrator windup, leading to large overshoot, slow settling time, and, sometimes, even instability in the system.[15] The traditional method to deal with the integrator windup problem is to tune the PID controller ignoring the actuator saturation and subsequently to add an anti-windup compensator to prevent the degradation of performance.[15–17]

One of the commonly used approaches is backcalculation (or tracking antiwindup).[16,17] As shown in Fig. 9, this approach consists of recomputing the integral term once the controller saturates. In particular, the integral value is reduced by feeding back the difference of the saturated u_s and unsaturated control signal u. Here T_t is the tracking time constant, and its value determines the rate at which the integral term is reset; its choice determines the performances of the overall control scheme. Some suggestions are to set $T_t = T_i$, but in some cases higher values can give further improvement in performance.[16,17]

Simulation Results

Simulations were performed with four different control approaches, that is, PID, PID with Smith prediction, PID with antiwindup, and PID with both Smith prediction and antiwindup. The average model obtained for PID control law design was used in the simulation. As just discussed, the thrust vector angle cannot be directly measured in a practical implementation of CFTV. In the present study, the corresponding vector angles are estimated based on the nearly linear relation between the thrust vector angle and the gap pressure such as that shown in Fig. 9 of Ref. 4 of the reference paper. This relationship is used here because it is based on extensive test results, which demonstrate that this pressure value is a reliable predictor of the vector angle. Because the pressure distributions along the collar obtained in the present test setup matched well with that of the reference paper, the use of the previously established correlation is well justified. Consequently, the uncertainty associated with the present vector angles is estimated to be similar to that associated with previous measurements in Ref. 4 and is approximately

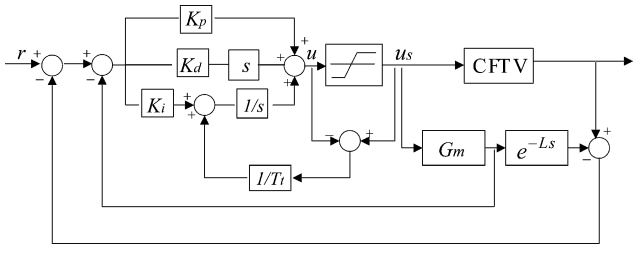

Fig. 9 Block diagram of an antiwindup Smith predictor.

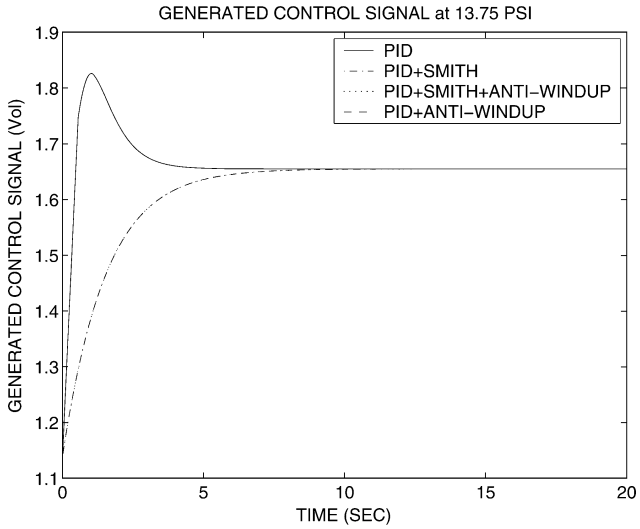

Fig. 10 Simulated controller performance at setpoint 13.75 psi: generated control signal.

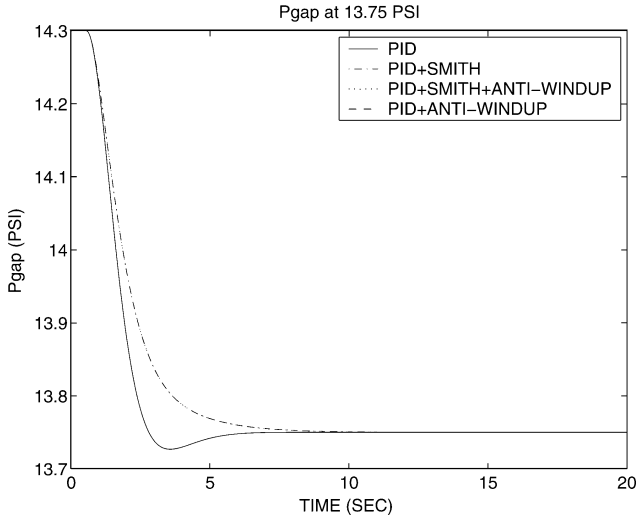

Fig. 11 Simulated controller performance at setpoint 13.75 psi: output signal.

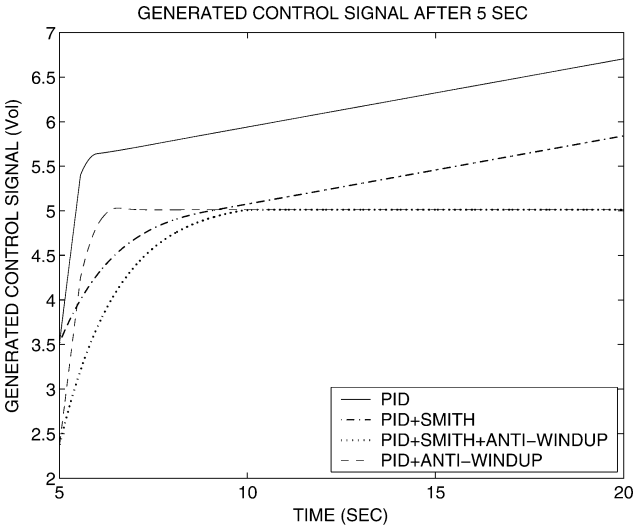

Fig. 12 Generated controller signal from setpoint 14.3 to 12.6 psi: 5 to 20 s.

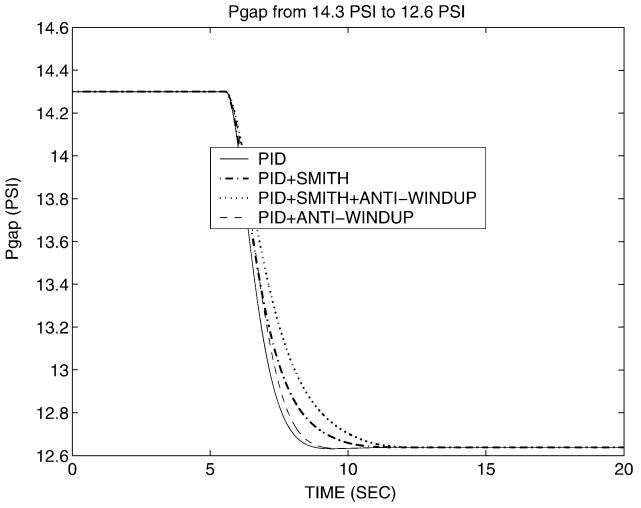

Fig. 13 Simulated controller performance from setpoint 14.3 to 12.6 psi.

±0.5 deg. The comparison of the controller performance was conducted under two cases: 1) without controller saturation and 2) with controller saturation.

In the first case, the CFTV system had a setpoint of 13.75 psi (corresponding to a 5.0-deg vector angle). In this case, antiwindup had no effect because all of the generated signals were within the working range of the control valve (i.e., [0 5] V). As shown in Fig. 10, the control signal generated from the PID controller overlapped with that of the PID controller with the antiwindup scheme, and the control signal generated from the Smith predictor overlapped with the PID controller with both the Smith predictor and the antiwindup scheme. Likewise, as shown in Fig. 11, the output signal resulting from the PID controller overlapped with that of the PID controller with the antiwindup scheme, and the output signal of the Smith predictor overlapped with PID controller with both the Smith predictor and the antiwindup scheme. Because the control signal generated by the Smith predictor was less aggressive than the corresponding PID controller, the Smith predictor did not cause overshoot, and the transient performance is smoother than the corresponding PID controller.

As an example of the second case, the CFTV system tracked a setpoint change from 14.3 to 12.6 psi (corresponding to an increase of thrust vector angle from 2.0 to 9.2 deg). Controller saturation occurred because of the dramatic change of the setpoint and the higher targeted setpoint at 12.6 psi. Figure 12 shows the generated control signal after the change of setpoint at 5 s. As shown in the figure, the control signal generated by the PID controller was above 5 V over most of the time period, the control signal generated by the PID controller with the Smith predictor was smaller but went beyond 5 V after 9.2 s. Antiwindup had the ability to avoid controller saturation; as shown in the figure, the control signals generated by the PID controller with the antiwindup scheme and the PID controller with both the Smith predictor and the antiwindup scheme were less than or equal to 5 V. The simulation was conducted with $1/T_t = 6/T_i$. It was observed that the higher the value of $1/T_t$, the stronger the antiwindup to avoid controller saturation. The simulated controller performance in Fig. 13 shows that with the current choice of T_t the Smith predictor was less aggressive than the corresponding PID antiwindup controller.

In the simulation results the Smith predictor did not show the desired advantage over the PID controller in compensating for the time delay and producing faster response times. The major reason for this is that the CFTV system is not time delay dominant (a system is said to have a dominant time delay if $L \geq 5T$) (Ref. 18). Simulations were conducted with increased time delay (e.g., L was increased to twice its original value), and it was seen that for PID control the longer time delay yielded a smaller phase margin, which led to large overshoot and very oscillatory behavior. For a large enough time delay (e.g., when the time delay was five times its original value for the CFTV system) the system became unstable. However, the performance of the Smith predictor was consistent as the time delay increased.

Experimental Results

Extensive experiments with the four different control approaches were conducted, and the performances of the different approaches were compared. Here, the experimental results under two types of reference signals are given.

In the case of a pulse reference signal, the desired collar gap pressure is 12.6 psi (corresponding to 9.2-deg thrust vector angle) from 0 to 20 s, 14.0 psi (corresponding to 3.7-deg thrust vector angle) from 20 to 40 s, and it is 13.0 psi (corresponding to 8.0-deg thrust vector angle) from 40 to 60 s. Figure 14 compares experimental outputs with different control approaches. Here both the dramatic changes of reference signal (from 12.6 to 14.0 psi, and from 14.0 to 13.0 psi) and the higher setpoint (12.6 psi) led to high control signal demands; thus, the PID controller always exhibited overshoot. The PID controller with the Smith predictor was always less aggressive, producing no overshoot while having a slower rise time than the PID controller alone. The PID controller with the antiwindup scheme had the ability to remove the overshoot while obtaining a similar rise time to that of the PID controller alone; here $T_t = T_i$ was used. The PID controller with both the Smith predictor and antiwindup scheme was less aggressive than the PID controller with the Smith predictor or the PID controller with the antiwindup, having a slower rise time.

In the case of a sine-wave reference signal, the desired collar gap pressure is described by $P_{\text{gap}} = 0.85 \sin(0.1\pi t + \pi/2) + 13.45$, corresponding to a maximum thrust vector angle of 9.2 deg and a minimum thrust vector angle of 2.0 deg. Figure 15 compares experimental outputs with different control approaches. Here, because of the continuous reference signal, control saturation occurred only when the reference signal was around 12.6 psi (where the generated control signal was lighter above 5 V) and 14.3 psi (where the generated control signal was slightly below 0 V). The PID controller with antiwindup was very close to the PID controller except around the instants of peak point 12.6 and 14.3 psi. The PID controller with the Smith predictor was less aggressive and had a slower response than the corresponding PID controller. The PID controller with both the Smith predictor and antiwindup scheme was very close to the PID controller with the Smith predictor. In all of the four cases, the closed-loop response exhibited obvious delay in tracking the reference signal. For example, the delay time for the PID controller to the reference sine wave signal was about 1.3 s.

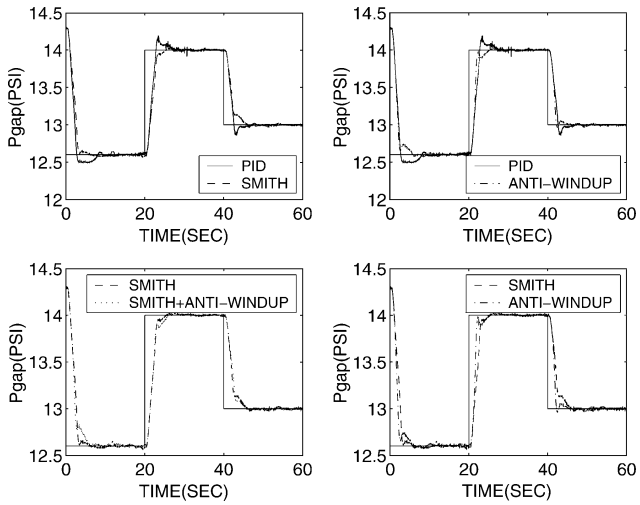

Fig. 14 Controller performance under a pulse reference signal.

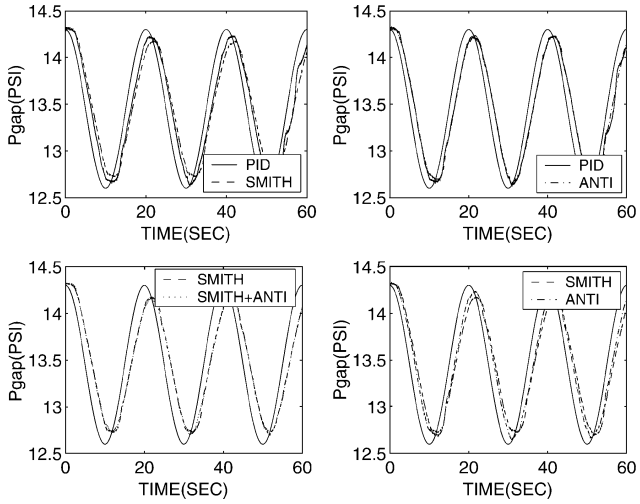

Fig. 15 Controller performance under a sine-wave reference signal.

In all of the experimental results, the four types of controllers demonstrated performance similar to the simulation results. In general, PID control with a Smith predictor eliminated the overshoot of the PID controller but increased the rise time and did not avoid controller saturation. PID control with antiwindup was effective in the presence of controller saturation. PID control with both a Smith predictor and antiwindup scheme did not show an advantage over PID control with only antiwindup. One reason for this is that, as just discussed, for a system such as CFTV that is not time delay dominant, a Smith predictor shows little or no advantage. In addition, a Smith predictor is model based, and the estimated model can be significantly different from the true CFTV model.

A PID controller with antiwindup is preferred in the current controller design. Extensive experimental results demonstrated the robustness of the PID controller under system uncertainties. However to further improve the system performance, an adaptive scheme that can update the system parameters and control parameters online should be investigated.

Conclusions

Counterflow thrust vectoring control is a promising technique for aircraft engine attitude control. Feedback control of Counterflow thrust vectoring (CFTV) is needed to obtain desired thrust vector angles by compensating for the transportation delay and parameter uncertainties.

This paper has described an experimental test bed for investigating feedback control of CFTV. System modeling was achieved using open-loop test data. A PID controller was developed for the system and was sometimes implemented with a Smith predictor and/or an antiwindup scheme. Then the performances of the PID controller, the PID controller with the Smith predictor, the PID controller with the antiwindup scheme, and the PID controller with both the Smith predictor and the antiwindup scheme were compared by both simulation and experimentation. Both simulation and experimental results demonstrated that the PID controller with antiwindup was the most effective control scheme.

This paper studied feedback control of one-dimensional CFTV in which only the pitch vectoring was considered. Open-loop, three-dimensional CFTV has been demonstrated in a laboratory setting. Feedback control of the three-dimensional CFTV will result in a multivariable control problem and, hence, is significantly more difficult than the corresponding single-input, single-output control problem considered here. The multivariable case will be studied in future research.

Acknowledgments

The authors would like to thank the U.S. Air Force Office of Scientific Research (Contract F49620-01-0550) for financial support for this research. We thank P. J. Strykowski for his invaluable help in design and constructing the experimental apparatus. We also thank Robert Avant, Fritz Dittus, and Mohammed I. Alidu for helping in the experimental setup.

References

[1] Alvi, F. S., Strykowski, P. J., Krothapalli, A., and Forliti, D. J., "Vectoring Thrust in Multiaxes Using Confined Shear Layers," *Journal of Fluids Engineering*, Vol. 122, No. 1, 2000, pp. 3–13.

[2]Maria, M., "Experimental Study on Counter-Flow Thrust Vector Control of a Subsonic Rectangular Nozzle," Florida State Univ., Technical Rept., Dec. 2000.

[3]Flamm, J. D., "Experimental Study of a Nozzle Using Fluidic Counterflow for Thrust Vectoring," AIAA Paper 98-3255, July 1998.

[4]Strykowski, P. J., Krothapalli, A., and Forliti, D. J., "Counterflow Thrust Vectoring of Supersonic Jets," *AIAA Journal*, Vol. 34, No. 11, 1996, pp. 2306–2314.

[5]Strykowski, P. J., and Krothapalli, A., "The Countercurrent Mixing Layer: Strategies for Shear-Layer Control," AIAA Paper 93-3260, July 1993.

[6]Van der Veer, M. R., "Counterflow Thrust Vectoring of a Subsonic Rectangular Jet," M.S. Thesis, Dept. of Mechanical Engineering, Univ. of Minnesota, Minneapolis, 1995.

[7]Su, C. Y., Stepanenko, Y., Svoboda, J., and Leung, T. P., "Robust Adaptive Control of a Class of Nonlinear Systems with Unknown Backlash-like Hysteresis," *IEEE Transactions on Automatic Control*, Vol. 45, No. 12, 2000, pp. 2427–2432.

[8]Astrom, K. J., and Hagglund, T., "The Future of PID Control," *Control Engineering Practice*, Vol. 9, No. 11, 2001, pp. 1163–1175.

[9]O'Dwyer, A., "The Estimation and Compensation of Process with Time Delays," Ph.D. Dissertation, School of Electronic Engineering, Dublin City Univ., Dublin, Aug. 1996.

[10]Huang, C. T., and Chou, C. J., "Estimation of the Underdamped Second-Order Parameters from the System Transient," *Industrial and Engineering Chemistry Research*, Vol. 33, No. 1, 1994, pp. 174–176.

[11]O'Dwyer, A., "PI and PID Controller Tuning Rules for Time Delay Processes: A Summary," Dublin Inst. of Technology, Technical Rept. AOD-00-01, Dublin, May 2000.

[12]Lee, D. K., Lee, M. Y., Sung, S. W., and Lee, I. B., "Robust PID Tuning for Smith Predictor in the Presence of Uncertain," *Journal of Process Control*, Vol. 9, No. 1, 1999, pp. 79–85.

[13]Aziz, K. I., and Thomson, M., "Minimal Controller Synthesis for Time-Delay Systems Using a Smith Predictor," *IEE Colloquium on Adaptive Controllers in Practice—Part Two, London*, March 1996, pp. 4/1–4/5.

[14]Hang, C. C., and Chong, B. W., "On Methods of Treating dc levels in an Adaptive Digital Smith Predictor," *IEEE Transactions on Automatic Control*, Vol. 35, No. 1, 1990, pp. 65, 66.

[15]Shine, H. B., "New Anti-Windup PI Controller for Variable-Speed Motor Drives," *IEEE Transactions on Industrial Electronics*, Vol. 45, No. 3, 1998, pp. 445–450.

[16]Visioli, A., "Modified Anti-Windup Scheme for PID Controllers," *IEE Proceedings—Control Theory Application*, Vol. 150, No. 1, 2003, pp. 49–54.

[17]Bohn, C., and Atherton, D. P., "An Analysis Package Comparing PID Anti-Windup Strategies," *IEEE Control System Magazine*, Vol. 15, No. 2, 1995, pp. 34–40.

[18]Rad, A. B., Tsang, K. M., and Lo, W. L., "Adaptive Control of Dominant Time Delay Systems via Polynomial Identification," *IEE Proceedings—Control Theory and Applications*, Vol. 142, No. 5, 1995, pp. 433–438.